ORIGINAL ARTICLE

Yunhao Tan
Jing Hua
Ming Dong

3D reconstruction from 2D images with hierarchical continuous simplices

Y. Tan · J. Hua (✉) · M. Dong
Department of Computer Science,
Wayne State University,
5143 Cass Avenue, 431 State Hall,
Detroit, MI, 48202, USA
{tanyunhao,jinghua,mdong}@wayne.edu

Abstract This paper presents an effective framework for the reconstruction of volumetric data from a sequence of 2D images. The 2D images are first aligned to generate an initial 3D volume, followed by the creation of a tetrahedral domain using the Carver algorithm. The resulting tetrahedralization preserves both the geometry and topology of the original dataset. Then a solid model is reconstructed using simplex splines with fitting and faring procedures. The reconstructed heterogenous volumetric model can be quantitatively analyzed and easily visualized. Our experiments demonstrated that our approach can achieve high accuracy in the data reconstruction. The novel techniques and algorithms proposed in this paper can be applied to reconstruct a heterogeneous solid model with complex geometry and topology from other visual data.

Keywords 3D reconstruction · DMS-splines · Hierarchical simplices · Data fitting

1 Introduction

The histopathological study of tissue is an important tool in the medical field for the prognosis of disease. Although informative in itself, histological slices are traditionally viewed under an optical microscope to reveal only a 2D image. One use for histology is the quantitative analysis of periprosthetic tissue due to wear debris-induced osteolysis, which is the most common cause of implant failure after total joint replacement. Since histological analysis cannot be applied non-invasively to humans, current diagnosis of aseptic loosening (AL) is still dependent on popular radiographic imaging; this method is not sufficient to accurately evaluate the complex 3D lesion of AL. A recent study by Looney et al. demonstrates that volumetric CT technology may be used as a measurement of periprosthetic osteolysis [15]. MicroCT (μCT) has been utilized to obtain 3D images for the quantitative assessment of bone in the osteolysis model. Preliminary studies have indicated that a correlation exists between 3D CT images and periprosthetic tissue histology, but it is extremely difficult to characterize the quantitative relation between CT-based volume data and microscopic periprosthetic tissue profile in order to provide accurate assessment of AL. It is of utter importance to map 3D volumetric CT data to 3D volumetric histology data in order to establish a mathematical model for the assessment of AL with non-invasive CT imaging. In this paper, we propose a method for the reconstruction of 2D optical histology images into a volumetric 3D histology image. This is achieved by properly transforming and arranging each histology slice in a sequential order to obtain a discretized volume. The procedure is referred as registration or alignment. Achieving the optimal transformation to minimize registration error is the biggest challenge in this procedure. Fundamentally, it requires a powerful data representation and a data fitting scheme based on the representation.

In the past few years, an unstructured volume representation has started to emerge as a viable modeling tool, where a tetrahedral mesh is exploited to dictate the domain of a volume [4, 5, 22, 25]. This type of representation is expected to become increasingly popular as modeling and visualization of geometric structures plus physical attributes of heterogeneous objects become common-

place. To satisfy the modeling requirement of high-order continuity in heterogeneous objects, volumetric modeling based on splines, such as B-splines or NURBS [11, 12, 16, 20, 23], appears to be more appropriate. Nonetheless, modeling with B-splines or NURBS has serious limitations. Its modeling scope is extremely constrained in term of geometric, topological, and attribute aspects.

We aim to design a representation with flexible, hierarchical continuous simplices. In order to reconstruct a heterogenous model of high accuracy, a unified volume modeling and reconstruction based on hierarchical trivariate DMS-splines is proposed in this paper. Our method has the following advantages:

– It explores the intrinsic image features of a histology section, making it a fully automatic procedure without human intervention during the reconstruction.
– Our model makes use of a more general and flexible tetrahedral domain, laying a foundation for both visualization and modeling tasks. The unstructured volume being modeled can be of complicated geometry and arbitrary topology.
– The trivariate DMS-spline-based representation offers a single, compact analytical representation, because it is a piecewise polynomial of the lowest possible degree and the highest possible continuity across the entire tetrahedral domain.
– This trivariate DMS-spline-based representation can also enable a strong multiresolution modeling capability through interactively subdividing any region of interest, allocating more knots and control points accordingly. The volume can be represented at desired resolution by extracting specific layers from the hierarchical simplices.
– Our method can adaptively refine the domain tetrahedra with hierarchical simplices, which introduces more degrees of freedom, leading to better fitting results.

We conduct extensive experiments using histology samples, and our empirical results demonstrate that the proposed paradigm significantly augments the current techniques within the medical, modeling, and visualization communities. Although we focus mainly on the volumetric reconstruction of the 3D histology image sequence for the biomedical domain, the applications of our technique are diverse, including material editing and reconstruction, volume simplification, data exploration and visualization in geological fields, and so on.

The paper is organized in the following way. Section 2 enumerates several milestones achieved by pioneers dedicated to this area. Section 3 contains the condensed theoretical principal of the DMS-spline and volumetric simplex splines as well, which are the mathematic models employed. Section 4 illustrates the tetrahedral domain exaction procedure that creates tetrahedral mesh for further use in modeling and reconstruction. Section 5 exhibits 3D volume reconstruction using simplex fitting and faring with hierarchical

simplices. Experiments and a discussion will be presented in Sect. 6 followed by a conclusion in Sect. 7.

2 Previous work

Much research effort from the medical imaging community has been devoted to establishing techniques for 3D histology analysis and visualization. Chan et al. proposed a methodology for making optimal registration decisions during 3D volume reconstruction [2]. A semi-automatic registration technique for 3D volume reconstruction from fluorescent laser scanning confocal microscope (LSCM) imagery was presented by Lee et al. [13]. They later proposed a fusion-based approach to address the problem of 3D volume reconstruction from depth adjacent subvolumes acquired using a confocal laser scanning microscope (CLSM) [14]. Tan et al. presented a feature curve-guided alignment algorithm to register microscopic slices based on the NURBS-based optimization of the extracted feature curves from the microscopic data [24]. Readers may find other relevant literature in [1, 3, 21].

Volume modeling and rendering via tetrahedral mesh has recently gained more popularity as well. Researchers are primarily interested in constructing or using the volumetric tetrahedral mesh dataset to achieve better rendering effects. Cignoni et al. [5] proposed a multi-resolution model for the representation and visualization of unstructured volumetric datasets based on a decomposition of the 3D domain into tetrahedra. Later, they presented a tetrahedral mesh simplification approach based on accurate error evaluation [4]. Roxborough and Nielson [22] presented a method for the visualization of freehand collected 3D ultrasound data based on adaptive, progressive construction of the tetrahedral mesh. A tetrahedral mesh structure to represent anatomical structures was adopted by Yao and Taylor [26]. They proposed an efficient and automatic algorithm to construct a tetrahedral mesh from contours in CT images. A rich body of previous work on tetrahedral meshes suggests that a simplicial complex is potentially promising to serve for both visualization and modeling.

Even though volume modeling using univariate splines, such as B-splines or NURBS, has received much attention from modeling and visualization communities in recent years [11, 16, 20, 23], multivariate simplex splines-based volume techniques based on a domain of simplices are less explored. They have only been extensively investigated in mathematical science. Motivated by an idea of Curry and Schoenberg for a geometric interpretation of univariate B-splines, de Boor [17] first presented a brief description of multivariate simplex splines. Since then, their theoretical perspectives have been explored extensively. From the blossoming point of view, Dahmen et al. [6] proposed triangular B-splines. Since then, Seidel and his colleagues demonstrated the practical feasibility of bivariate DMS-splines in graphics and shape design in [8, 19]. In sharp

contrast to theoretical advances, the application of trivariate simplex splines has been severely under-explored. Hua et al. [9] initiated using simplex splines for heterogeneous solid modeling and derived several theoretical formula for fast rendering of the simplex spline volumes. Recently, Rössl et al. [17] presented a novel approach to reconstruct volume from structured grid data samples using trivariate quadric super splines defined on a uniform tetrahedral partition. They used Bernstein–Bézier techniques to compute and evaluate the trivariate spline and its gradient. Moreover, the exact intersection for a ray and prescribed isovalue can be easily determined in an analytic and exact way. The major difference between Rössl et al.'s method and ours lies in the following:

– Our method uses arbitrary tetrahedral domains instead of regular ones.
– Our method uses a general trivariate DMS-spline of degree $n \geq 2$, which has more degrees of freedom (control points and knots); the continuity between adjacent tetrahedra can be easily maintained because of the optimal smoothness of DMS-splines.
– Our method uses hierarchical structures to model level-of-details.

3 Trivariate DMS-spline volumes

First, let us review some theoretical background of the trivariate DMS-spline volume, the mathematic model employed in our unified framework.

A degree n trivariate simplex spline, $M(x|x_0, \ldots, x_{n+3})$, can be defined as a function of $x \in \mathbb{R}^3$ over the half open convex hull of a point set $V = [x_0, \ldots, x_{n+3}]$, depending on the $n + 4$ knots $x_i \in \mathbb{R}^3$, $i = 0, \ldots, n+3$. The trivariate simplex splines may be formulated recursively, which facilitates point evaluation and its derivative and gradient computation. When $n = 0$,

$$M(x|x_0, \ldots, x_3) = \begin{cases} \frac{1}{|\text{Vol}_{\mathbb{R}^3}(x_0, \ldots, x_3)|}, & x \in [x_0, \ldots, x_3), \\ 0, & \text{otherwise}, \end{cases}$$

and when $n > 0$, select four points $W = \{x_{k_0}, x_{k_1}, x_{k_2}, x_{k_3}\}$ from V, such that W is affinely independent, then

$$M(x|x_0, \ldots, x_{n+3}) = \sum_{j=0}^{3} \lambda_j(x|W) M(x|V \setminus \{x_{k_j}\}), \quad (1)$$

where $\sum_{j=0}^{3} \lambda_j(x|W) = 1$ and $\sum_{j=0}^{3} \lambda_j(x|W)x_{k_j} = x$.

The directional derivative of $M(x|V)$ with respect to a vector d is defined as follows:

$$D_d M(x|V) = n \sum_{j=0}^{3} \mu_j(d|W) M(x|V \setminus \{x_{k_j}\}), \quad (2)$$

where $\sum_{j=0}^{3} \mu_j(d|W)x_{k_j} = x$ and $\sum_{j=0}^{3} \mu_j(d|W) = 0$.

Now let T be an arbitrary "proper"[1] tetrahedralization of the bounded domain $D \subset \mathbb{R}^3$. To each vertex t of the tetrahedralization, we assign a knot cloud, which is a sequence of points $[t_0, t_1, \ldots, t_n]$, where $t_0 \equiv t$. For every tetrahedron $I = (p, q, r, s)$, we require that

– all the tetrahedra $[p_i, q_j, r_k, s_l]$ with $i + j + k + l \leq n$ are non-degenerate;
– the set

$$\Omega = \text{interior}\left(\bigcap_{i+j+k+l \leq n} [p_i, q_j, r_k, s_l] \right) \neq \varnothing \quad (3)$$

is not empty;
– if I has a boundary triangle, the knots associated to the boundary triangle must lie outside of the domain.

We then define, for each tetrahedron I and $i + j + k + l = n$ (in the following, we use β to denote 4-tuple (i, j, k, l)), the knot sets

$$V_\beta^I = [p_0, \ldots, p_i, q_0, \ldots, q_j, r_0, \ldots, r_k, s_0, \ldots, s_l]. \quad (4)$$

The basis functions of normalized DMS-splines are then defined as

$$N_\beta^I(u) = |\det(p_i, q_j, r_k, s_l)| M(u|V_\beta^I). \quad (5)$$

Assuming Eq. 3, these basis functions can be shown to be all non-negative and to form a partition of unity. The trivariate DMS-spline volume is the combination of a set of basis functions with control points c_β^I:

$$s(u) = \sum_{I \in T} \sum_{|\beta| = n} c_\beta^I N_\beta^I(u). \quad (6)$$

The *generalized* control points c_β^I are now $(m + 3)$ vectors, including control points (p^x, p^y, p^z) for the solid geometry, and control coefficients $(g^1, \ldots, g^m)$ for the attributes, where m denotes the number of attributes associated with the geometry. For the complete description of trivariate DMS-spline volumes, readers are referred to [6, 9, 10].

4 Tetrahedral domain construction

In our volume reconstruction algorithm, we plan to employ trivariate DMS-splines as the representation due to its attractive properties described before. The first important step is to construct a good initial tetrahedralization basis for the later data fitting and faring steps. When starting with a good initial tetrahedralization, the later

---

[1] Here, "proper" means that every pair of domain tetrahedra are disjoint, or share exactly one vertex, one edge, or one face.

refinement computation will be greatly reduced. Good initial domain tetrahedralization should preserve both geometric and attribute features of the original volume dataset.

4.1 Initial alignment of 2D slices

Before the structure of 3D histology can be explored and analyzed, generating a high-fidelity 3D volume is a crucial and preliminary step in which all histology slices need to be stacked into one volume. The grid data structure can be employed here and we choose the Analyze 7.5 file format, which is already a well-established industry standard.

First, 2D histology slices are scanned into the computer through a digital histology film scanner. This high resolution equipment can produce quality images with detailed cell structures. In this step, necessary image processing filters, for instance, the Gaussian smoother, will be applied to the raw data due to the inevitable noises. Figure 1 shows a part of a sequence of 2D images scanned from a histology sectioning profile.

Between two neighboring histology sections, there is no high-order discontinuity in the structure, i.e., there exists substantial similarities, which can be used to match adjacent slices. Based on this observation, we need to minimize the following equation:

$$\min DIFF_{\text{den}} = \sum_{i=1}^{n-1} \|I(i) - T \cdot I(i+1)\|^2, \tag{7}$$
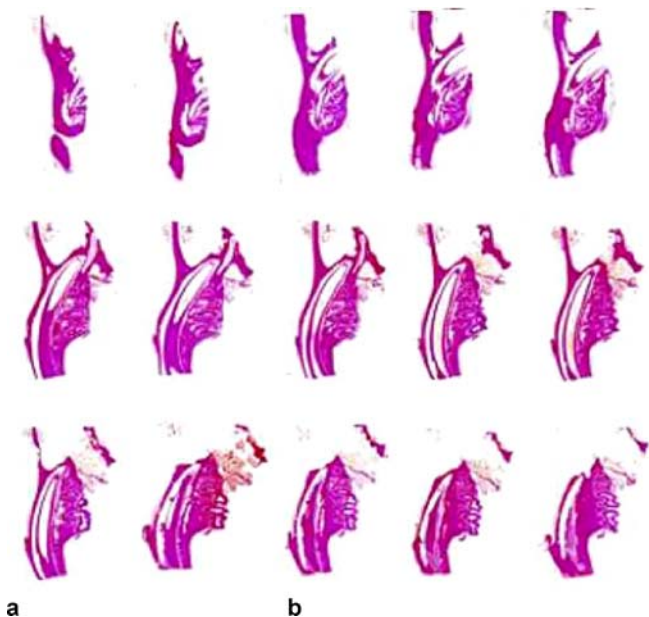
Fig. 1. A part of a sequence of 2D images scanned from a histology sectioning profile. Histology structures gradually change from slice to slice

where $I(i)$ indicates the density distribution of the i-th slice. $I(i+1)$ is subject to the affine transformation matrix T. Here we select the i-th slice as the stationary one, and apply affine transformation to the $(i+1)$-th slice. The correspondent affine transformation T is a 4×4 matrix as below:

$$\begin{bmatrix} x' \\ y' \\ z' \\ 1 \end{bmatrix} = T \begin{bmatrix} x \\ y \\ z \\ 1 \end{bmatrix}, \tag{8}$$

where

$$T = \begin{bmatrix} t_{00} & t_{01} & t_{02} & t_{03} \\ t_{10} & t_{11} & t_{12} & t_{13} \\ t_{20} & t_{21} & t_{22} & t_{23} \\ t_{30} & t_{31} & t_{32} & t_{33} \end{bmatrix},$$

and $\begin{bmatrix} x \\ y \\ z \\ 1 \end{bmatrix}$ denotes the original position of a voxel and $\begin{bmatrix} x' \\ y' \\ z' \\ 1 \end{bmatrix}$

denotes the transformed position. Because we use homogeneous coordinates here, the position vector in Eq. 8 is extended to order 4. Here T is a combination of rotation factor and translation factor. Equation 7 is essentially a least squares problem. Solving this system, we can obtain a set of transformations that construct an initial alignment of all 2D histology sections.

4.2 The Carver algorithm for tetrahedralization

Constraint Delaunay tetrahedralization (CDT) [7] is the most widely used algorithm to construct a tetrahedral mesh. However, CDT works great only for those models from which corresponding isosurfaces can be explicitly extracted, i.e., those with simple geometry. To increase the versatility of our framework, we develop another algorithm for models without such well-defined isosurfaces, e.g., histology models. The algorithm fulfills the objective in two major steps: 1) arbitrary Delaunay tetrahedralization, and 2) outside tetrahedra removal using the Carver algorithm. The detailed steps of our algorithm are described as follows:

1. From Sect. 4.1, what we obtain is a structured grid volume. The first step here is to down-sample the volume to get finite discretized points, which are the later vertices of the tetrahedral domain. It is intuitive that we shall have more tetrahedra in the feature area. More points in feature-dense areas and less points in uniform areas are selected according to the voxels' intensity variation levels. Here, we simply use gradients of physical attributes as the level stated. Figure 2a shows the discretized point sets.
2. Then we use the points selected from the initial volume as the vertices input of *genus-zero* Delaunay

tetrahedralization. After arbitrary Delaunay tetrahedralization, the initial *genus-zero* tetrahedral mesh is retrieved with the convex hull of the vertices as its boundary mesh. Accordingly, more tetrahedra will be created in the feature area due to more vertices presented and vice versa. Figure 2b is the mesh created by arbitrary Delaunay tetrahedralization.

3. Starting from one user specified tetrahedron, neighboring tetrahedra will be removed recursively. Those removed tetrahedra form another object, namely the "OUTSIDER", and we only need to detect the neighboring tetrahedra of its boundary. The criteria for stopping is that there are no additional tetrahedra to be added to the "OUTSIDER".

4. The Carver algorithm yields tetrahedra of arbitrary topology. Islands should be removed based on the fact that histology may be of any topology, but its geometric feature is continuous anywhere. Islands are mostly caused by inevitable noise from original data set. Figure 2c shows the tetrahedral mesh after 2 removal steps, with volume presented. Figure 2d shows the initial mesh after islands have been removed.

5 Volume reconstruction

To model the histology attribute over the simplex spline-based volume, it is much more desirable to have a fitting
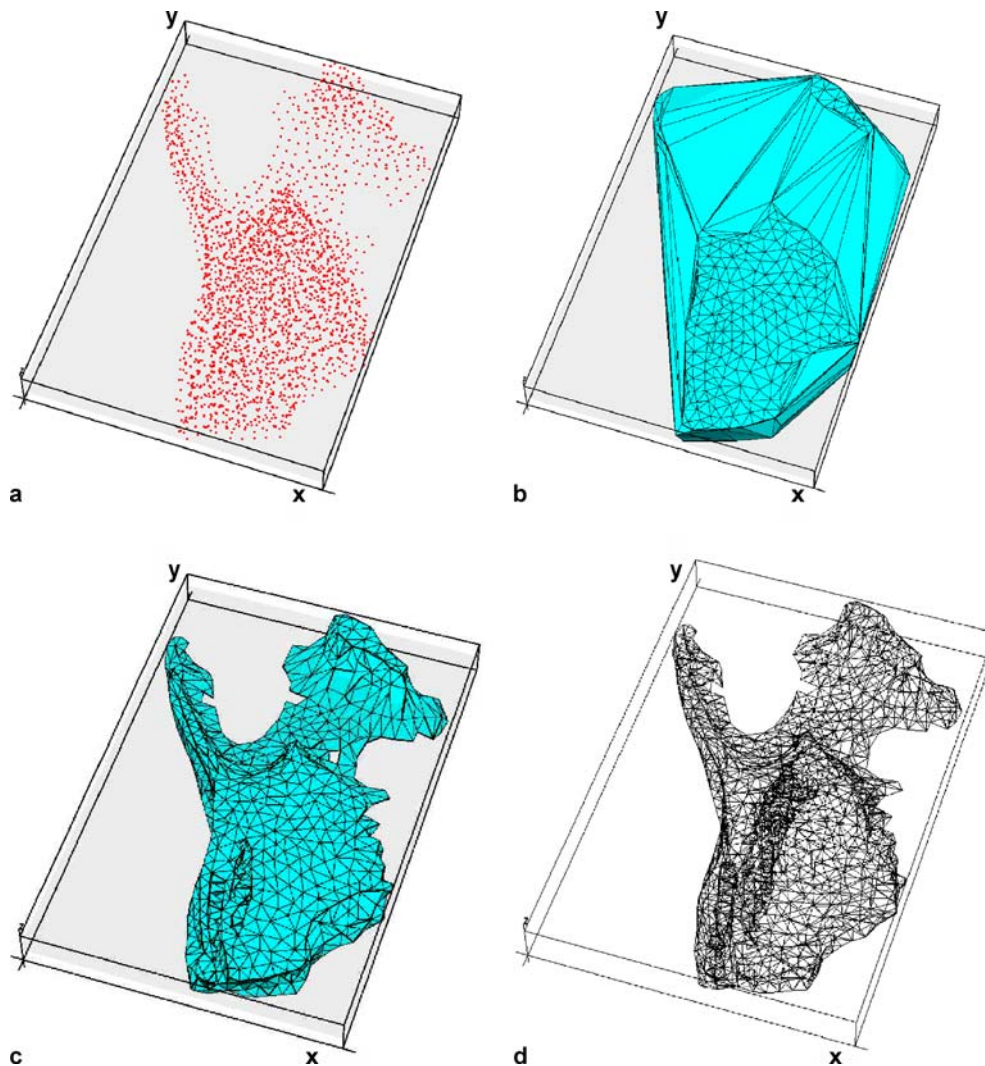
Fig. 2a–d. a Point set down-sampled as input of Delaunay tetrahedralization. **b** Arbitrary Delaunay tetrahedralization with a convex hull as its boundary mesh. **c** The Carver algorithm removes outside tetrahedra from the tetrahedral domain. **d** Initial mesh after islands removal

tool that converts the discrete volume data to continuous splines. In this section, we propose a method for volume reconstruction using DMS-splines.

5.1 Hierarchical DMS-spline volumes

Before we introduce the hierarchical DMS-spline volumes, let us first review some results on a triangular B-spline.

Theorem 1 (Piecewise polynomial representation [17]**).** *Let F be any piecewise polynomial of degree n over a given triangulation T, and let F_I be the restriction of F to the triangle $\Delta(I)$ and f_I be the polar form of F_I. Then the following identity holds for all $\boldsymbol{u}$:*

$$F(\boldsymbol{u}) = \sum_{I \in I} \sum_{|\beta|=n} f_I(\,) N_\beta^I(\boldsymbol{u}). \tag{9}$$

For more information about the polar form, we refer the readers to [17, 18].

The above theorem holds for a general $s(\geq 2)$-variate DMS-spline. Let I be the tetrahedron of interest in the domain of $\boldsymbol{s}(\boldsymbol{u})$, and we want to add more degrees of freedom in I to model the details. There are two different ways to solve this problem. The first is knot insertion, in which one knot is inserted into the tetrahedron I, and I is subdivided into four tetrahedra. Multiple knots can be inserted one by one. The second is hierarchical structures by building a new spline $\boldsymbol{s}_I^1(\boldsymbol{u})$, whose domain is a regularly subdivided tetrahedra of I. The major differences between knot insertion and hierarchical structures (see Fig. 3) are as follows:

- Hierarchical structures need the additional splines $\boldsymbol{s}_I^1(\boldsymbol{u})$, but do not change the original spline $\boldsymbol{s}(\boldsymbol{u})$, while knot insertion does affect the spline $\boldsymbol{s}(\boldsymbol{u})$.
- Hierarchical structures need a special technique to maintain a certain continuity between the original spline and new spline, while knot insertion does not.
- Knot insertion might introduce poor quality tetrahedra, while hierarchical structures do not.
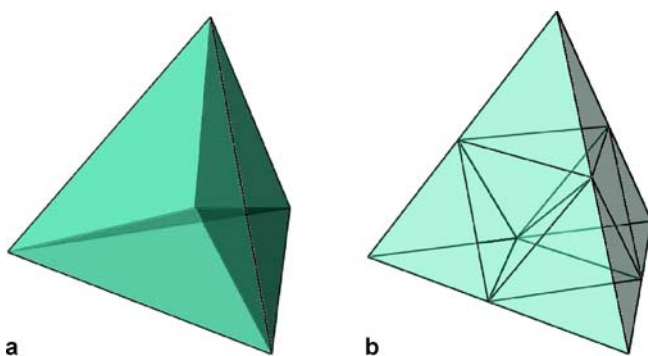
Fig. 3. a Knot insertion. **b** Hierarchical simplices

In order to maintain certain continuity between $\boldsymbol{s}_{\boldsymbol{u}}^1$ and $\boldsymbol{s}_{\boldsymbol{u}}$, they must have "overlays". Unlike the tensor-product B-splines, which usually extend the domain one level to maintain C^1-continuity between the two layers, we use the boundary tetrahedra as the overlays, which means the control points and knots inside these tetrahedra are fixed. The detailed hierarchical simplices construction is as follows:

1. Subdivide I to a user-specified level.
2. Compute all the control points in the domain I by Eq. 9.
3. Set all the control points and knots associated to the boundary tetrahedra to be fixed and others to be free.

Note that the refinement (1–3) produces the exact presentation of the original splines. Recall that movement of a free control point c_β^I only influences the splines on the tetrahedron $\Delta(J)$ and on the tetrahedra directly surrounding $\Delta(J)$. Since we fix the control points and knots of the boundary tetrahedra, any change of internal control points will not affect the function value and gradient across the boundary. Thus, we maintain C^1-continuity between the new spline and the original one.

For a better understanding, we illustrate the above scheme with an example of a triangular B-spline surface. Figure 4a is the original surface and the marked area is the region of interest to be refined. In Fig. 4c, we construct another triangular B-spline surface that represents the marked area exactly. This new surface has refined domain triangulation and more control points. In Fig. 4e, we move a free control point of the new surface and the two surfaces still blend smoothly. Note that the surfaces in Figures 4c and 4e use the same domain.

5.2 Volume reconstruction problem statement

The problem of volume reconstruction can be stated as follows: given a set $P = \{\boldsymbol{p}_i\}_{i=1}^m$ of points $\boldsymbol{p}_i = (x_i, y_i, z_i, d_i) \in \mathbb{R}^4$, find a trivariate DMS-spline volume $s : \mathbb{R}^3 \to \mathbb{R}^4$ that approximates P.

Since we are interested only in reconstructing the data from attributes, our trivariate DMS-spline volumes are scalar functions, i.e., the control points $c_\beta^I \in \mathbb{R}$ are scalar values. Unlike the existing fitting algorithms with parametric representations, which usually find a one-to-one mapping between the data points and the points in the parametric space, our method skips this parameterization procedure. As stated in Sect. 4, we first construct a tetrahedralization parametric domain that is close to the original geometry of the to-be-fitted dataset. We use the position (x_i, y_i, z_i) of the data point $\boldsymbol{p}_i$ as its parametric value. Therefore, we need to minimize the following objective function:

$$\min E(F) = E_{\text{dist}}(s) + \lambda \cdot E_{\text{fair}}(s), \tag{10}$$
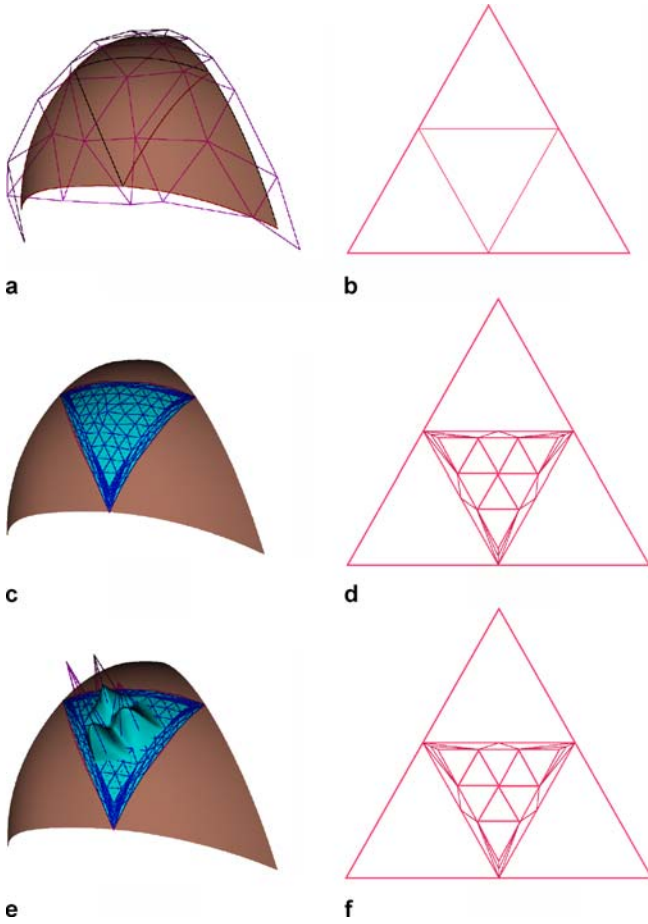
Fig. 4a–f. Illustration of hierarchical bivariate DMS-spline surfaces. **a** A bivariate DMS-spline surface. **b** Corresponding domain triangulation of **a**. **c** Hierarchical structure of one domain triangle of **a**. **d** Corresponding domain triangulation of **c**. **e** Moving the free control points will not affect the continuity across the boundary. **f** Corresponding domain triangulation of **e**

where

$$E_{\text{dist}}(s) = \sum_{i=1}^{m} (d_i - s(x_i, y_i, z_i))^2, \qquad (11)$$

and $E_{\text{fair}}(s)$ is a fairness function with the smoothing factor $\lambda \geq 0$.

The most commonly-used fairness functions, such as simplified membrane energy and thin-plate energy, require integration, which is usually computationally intensive. In this paper, we use a simple, yet effective, fairness function:

$$E_{\text{fair}}(s) = \sum_{i=1}^{m} (n_i \cdot s(x_i, y_i, z_i))^2, \qquad (12)$$

where n_i is the gradient at point (x_i, y_i, z_i). Note that these gradients can be calculated by local least-squares fitting to P.

5.3 Hierarchical fitting

The above volume data fitting procedure attempts to minimize the total squared distance of the volume data points d_i to the DMS-spline $s(u)$. For some regions with very dense points or sharp features, it is often desirable to introduce new degrees of freedom into the spline representation in order to improve the fitting quality. Hierarchical structures are suitable for this purpose.

If the error metric inside a tetrahedron I is greater than a user-specified value, and it contains enough points, e.g., $8 * N_{\min}$ in our implementation, we construct the hierarchical DMS-splines $s_I^{(1)}(u)$ on I as follows:

1. Shrink I slightly and get a smaller tetrahedron J. Denote $I \setminus J$ the narrow band between I and J.
2. Subdivide J into 8 tetrahedra.
3. Perform tetrahedralization for the narrow band between I and J.
4. Compute the control points of $s_I^{(1)}(u)$ by Eq. 9.
5. Fix the control points and knots associated to the tetrahedra in the band $I \setminus J$ and let others be free.
6. For all the data points inside I, define $e_i = d_i - s(x_i, y_i, z_i)$.
7. Solve $E_{\text{dist}}^I = \sum_{(x_i, y_i, z_i) \in I} (e_i - s_I^1(u))^2$ with the free control points and knots.

This refinement step is called repeatedly until the stopping criteria are satisfied. Then the output of our volume reconstruction is a series of trivariate DMS-splines; i.e., to evaluate $u \in \Delta I$, we use

$$s(u) = s^0 u + s_I^1(u) + s_I^2(u) + \dots$$

The number of levels needed in the evaluation depends on the application.

Although the base domain tetrahedron contains enough points, the number of data points in some subdivided tetrahedra may be less than $N_{\min}$ due to the nature of the unstructured data. If this happens, we also fix the control points inside the small tetrahedra to avoid the underdetermined problem.

In order to improve the performance of our fitting method, we start with a down-sampled dataset in the coarse level and consider the whole dataset in the fine level. For example, when fitting the rat tooth data, we use 64 572 points in level 0 to reconstruct the rough geometry and density, and use 350 000 points in level 2 to reconstruct the details.

Table 1. Statistics of 3D reconstruction

Sample	Continuous simplices (num.)	Fitting error
1	10 231	1.878×10^{-4}
2	12 855	1.526×10^{-4}

6 Experiments and discussion

We implemented a prototype system on a PC with 2.8 GHz P4 CPU and 2 GB of RAM. The system is written in VC++ and VTK 4.2. Table 1 shows the performance statistics of our fitting algorithm on several datasets, where the fitting error is the root-mean-square error. With the help of hierarchical simplices, our volume reconstruction algorithm can achieve very good results. The entire 3D re-construction procedure from 2D histology sequences takes a few hours to complete.

Through our framework, aseptic loosening at rat apical root can be examined and compared by quantifying the reconstructed 3D histology data. We also propose a scheme to analyze the aseptic loosening region of interest by comparing histology data with μCT data. Bone resorption can be measured along a time axis. Figure 5 shows an example. Because histology and μCT are different modali-
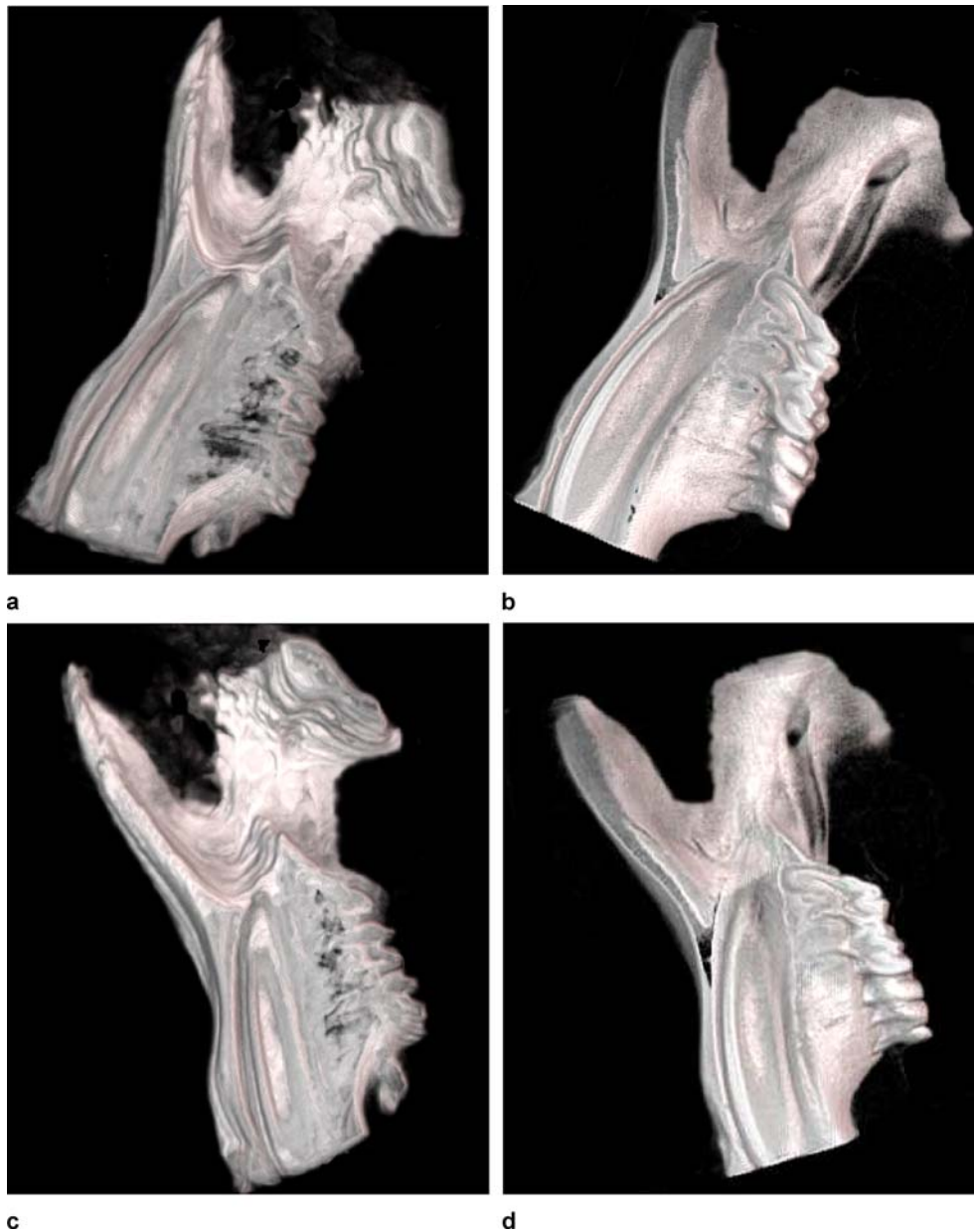
Fig. 5. a 3D visualization of reconstructed 3D histology volume after similarity mapping. **b** 3D visualization of the corresponding μCT volume from the same viewpoint. **c** 3D Visualization of reconstructed 3D histology volume after global faring. **d** 3D visualization of corresponding μCT volume from the same viewpoint

ties, necessary registration will be acquired before such an analysis, to make the comparison substantial.

7 Conclusion

In this paper, we have articulated a new integral approach for representing, modeling, and reconstructing volume data. In particular, we employ a hierarchical trivariate simplex spline model that is defined over a hierarchical and progressive tetrahedralization of arbitrary 3D domains. Our framework supports both structured and unstructured data. The modeled volume can be of complicated geometry and arbitrary topology. We have developed a new paradigm to reconstruct non-discrete models from a sequence of 2D images. With the flexible hierarchical struc-

tures, our method can adaptively refine the domain tetrahedralization and introduce more degrees of freedom locally for better fitting results. The volumes can then be re-modeled and re-edited by manipulating the control vectors and/or associated knots of trivariate simplex splines easily. Our results demonstrate that the proposed paradigm augments the current tetrahedral representation and reconstruction techniques with new and unique advantages that can be applied to diverse research areas.

References

1. Bardinet, E., Ourselin, S., Malandain, G., Tande, D., Parain, K., Ayache, N., Yelnik, J.: Three dimensional functional cartography of the human basal ganglia by registration of optical and histological serial sections. In: Proceedings of IEEE International Symposium on Biomedical Imaging, pp. 329–332 (2002)
2. Chan, H., Chung, A.: Efficient 3D–3D vascular registration based on multiple orthogonal 2D projections. In: Second International Workshop on Biomedical Image Registration (WBIR 2003), vol. 2717, pp. 301–310. Springer (2003)
3. Choi, S., Lee, J., Kim, J., Kim, M.: Volumetric object reconstruction using the 3D-MRF model-based segmentation. IEEE Trans. Med. Imaging **16**(6), 887–892 (1997)
4. Cignoni, P., Constanza, D., Montani, C., Rocchini, C., Scopigno, R.: Simplification of tetrahedral meshes with accurate error evaluation. In: Proceedings of the Conference on Visualization '00, pp. 85–92. IEEE Computer Society (2000)
5. Cignoni, P., De Floriani, L., Montani, C., Puppo, E., Scopigno, R.: Multiresolution modeling and visualization of volume data based on simplicial complexes. In: Proceedings of the 1994 Symposium on Volume Visualization, pp. 19–26 IEEE Computer Society (1994)
6. Dahmen, W., Micchelli, C.A., Seidel, H.: Blossoming begets B-spline bases built better by b-patches. Math. Comput. **59**(199), 97–115 (1992)
7. Edelsbrunner, H.: Geometry and Topology for Mesh Generation. P.G. Ciarlet, A. Iserles, R.V. Kohn, M.H. Wright, eds. Cambridge University Press (2001)
8. Greiner, G., Seidel, H.: Modeling with triangular B-splines. IEEE Comput. Graph. Appl. **14**(2), 56–60 (1994)
9. Hua, J., He, Y., Qin, H.: Multiresolution heterogeneous solid modeling and visualization using trivariate simplex

splines. In: Proceedings of the Ninth ACM Symposium on Solid Modeling and Applications, pp. 47–58 (2004)
10. Hua, J., He, Y., Qin, H.: Trivariate simplex splines for inhomogeneous solid modeling in engineering design. ASME Trans. J. Comput. Information Sci. Eng. **5**(2), 149–157 (2005)
11. Hua, J., Qin, H.: Haptics-based volumetric modeling using dynamic spline-based implicit functions. In: Proceedings of IEEE Symposium on Volume Visualization and Graphics, pp. 55–64 (2002)
12. Hua, J., Qin, H.: Haptics-based dynamic implicit solid modeling. IEEE Trans. Vis. Comput. Graph. **10**(5), 574–586 (2004)
13. Lee, S., Bajcsy, P.: Feature based registration of fluorescent LSCM imagery using region centroids. In: Proceedings of SPIE International Symposium in Medical Imaging, vol. 5747, pp. 170–181 (2005)
14. Lee, S., Bajcsy, P.: Three-dimensional volume reconstruction based on trajectory fusion from confocal laser scanning microscope images. In: Proceedings of IEEE Conference on Computer Vision and Pattern Recognition(CVPR 06), vol. 2, pp. 2221–2228 (2006)
15. Looney, R., Boyd, A., Totterman, S., Seo, G., Tamez-Pena, J., Campbell, D., Novotny, L., Clcott, C., Martell, J., Hayes, F., O'Keefe, R., Schwarz, E.: Volumetric computerized tomography as a measurement of periprosthetic acetabular osteolysis and its correlation with wear. Arthritis Res. **4**(1), 59–63 (2002)
16. Martin, W., Cohen, E.: Representation and extraction of volumetric attributes using trivariate splines: A mathematical framework. In: Proceedings of the 7th ACM Symposium on Solid Modeling and Applications, pp. 234–240 (2001)
17. Pauly, M., Gross, M., Kobbelt, L.: Efficient simplification of point-sampled surfaces. In: IEEE Visualization 02 Proceedings pp. 163–170 (2002)

18. Pauly, M., Keiser, R., Kobbelt, L., Gross, M.: Shape modeling with point-sampled geometry. In: SIGGRAPH 03 Proceedings pp. 641–650 (2003)
19. Pfeifle, R., Seidel, H.: Fitting triangular B-splines to functional scattered data. In: Proceedings of Graphics Interface '95, pp. 80–88 (1995)
20. Raviv, A., Elber, G.: Three dimensional freeform sculpting via zero sets of scalar trivariate functions. In: Proceedings of 5th ACM Symposium on Solid Modeling and Applications, pp. 246–257 (1999)
21. Rosa, R., Chirco, P., Massari, R.: Reconstruction corrections in advanced neutron tomography algorithms. IEEE Trans. Nucl. Sci. **52**(1), 400–403 (2005)
22. Roxborough, T., Nielson, G.M.: Tetrahedron based, least squares, progressive volume models with application to freehand ultrasound data. In: Proceedings of the conference on Visualization'00, pp. 93–100 (2000)
23. Schmitt, B., Pasko, A., Schlick, C.: Constructive modeling of FRep solids using spline volumes. In: Proceedings of the 6th ACM Symposium on Solid Modeling and Applications, pp. 321–322 (2001)
24. Tan, Y., Hua, J., Dong, M.: Feature curve-guided volume reconstruction from 2D images. In: Proceedings of IEEE International Symposium on Biomedical Imaging (2007)
25. Trotts, I., Hamann, B., Joy, K.: Simplification of tetrahedral meshes with error bounds. IEEE Trans. Vis. Comput. Graph. **5**(3), 224–237 (1999)
26. Yao, J., Taylor, R.: Tetrahedral mesh modeling of density data for anatomical atlases and intensity-based registration. In: Proceedings of the Third International Conference on Medical Image Computing and Computer-Assisted Intervention, pp. 531–540 (2000) LSCM imagery
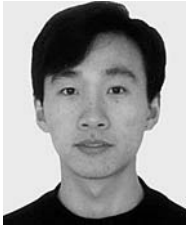
YUNHAO TAN is a Ph.D. student in the Department of Computer Science at Wayne State University and a research assistant in the Graphics and Imaging Laboratory. He received his BS degree from Beijing Information Technology Institute in 2001, then he worked for the Beijing Bear Technology Group as a software engineer till 2003. His research interests include computer graphics, visualization and solid modeling. He is a student member of IEEE.

DR. JING HUA is an assistant professor of computer science at Wayne State University and the Director of the Graphics and Imaging Lab. He received his PhD degree (2004) in computer science from the State University of New York at Stony Brook. He also received his MS degree (1999) in pattern recognition and artificial intelligence from the Institute of Automation, the Chinese Academy of Sciences in Beijing, P.R. China. His research interests include computer graphics, geometric computing and 3D image analysis. Dr. Hua is as an Editorial Board Member for the International Journal of Technology Enhanced Learning and is a program committee member for many international conferences. He is a member of the IEEE and ACM.

MING DONG received his BS degree from Shanghai Jiao Tong University, Shanghai, P.R. China in 1995 and his PhD degree from the University of Cincinnati, Ohio, in 2001, both in electrical engineering. He joined the faculty of Wayne State University, Detroit, MI in 2002. He is currently an assistant professor of computer science and a scientific member of Developmental Therapeutics Program, Karmanos Cancer Institute. He is also the Director of the Machine Vision and Pattern Recognition Laboratory in the Department of Computer Science. His research interests include pattern recognition, multimedia analysis, and data mining. He is an associate editor of the Pattern Analysis and Applications Journal and is on the editorial board of International Journal of Technology Enhanced Learning.